Supplementary File

Article's Title;

Physiologically Based Pharmacokinetic Modeling of Bosentan Identifies the Saturable Hepatic Uptake as A Major Contributor to Its Nonlinear Pharmacokinetics

Authors;

Masanobu Sato, Kota Toshimoto, Atsuko Tomaru, Takashi Yoshikado, Yuta Tanaka, Akihiro Hisaka, Wooin Lee and Yuichi Sugiyama

Journal Title;

Drug Metabolism and Disposition

Supplementary text 1

In our constructed PBPK model, the concentration profile of bosentan in each compartment can be expressed by the following differential equations.

Central:

$$V_c \frac{dC_c}{dt} = Q_h(C_{EH5} - C_c) + Q_a\left(\frac{C_a}{K_{p,a}} - C_c\right) + Q_m\left(\frac{C_m}{K_{p,m}} - C_c\right) + Q_s\left(\frac{C_s}{K_{p,s}} - C_c\right) - CL_r\, C_c$$

(V, volume; C, concentration; Q, blood flow rate of each organ; subscript c, h, a, m, and s, the compartment of central, hepatic, adipose, muscle and skin, respectively; EH5, the fifth extrahepatic compartment)

Hepatocyte compartments 1 to 5:

$$\frac{1}{5}V_{HCi}\left(\frac{dC_{HCi}}{dt}\right) = \frac{1}{5}\left\{(PS_{act} + PS_{dif,inf})f_B C_{HEi} - (PS_{dif,eff} + CL_{int,met})f_H C_{HCi}\right\}$$

Hepatic extracellular compartment 1:

$$\frac{1}{5}V_{HE1}\left(\frac{dC_{HE1}}{dt}\right) = Q_h(C_c - C_{HE1}) + \frac{1}{5}\left\{PS_{dif,eff}f_H C_{HC1} - (PS_{act} + PS_{dif,inf})f_B C_{HE1}\right\}$$

(HC1, the first hepatocellular compartment; f_B, the unbound fraction in blood)

Hepatic extracellular compartments 2 to 5:

$$\frac{1}{5}V_{HEi}\left(\frac{dC_{HEi}}{dt}\right)$$

$$= Q_h\left(C_{HE(i-1)} - C_{HEi}\right)$$

$$+\frac{1}{5}\left\{PS_{dif,eff}f_H C_{HCi} - (PS_{act} + PS_{dif,inf})f_B C_{HEi}\right\}$$

(subscript i, the number of the compartment)

Non-elimination organ (adipose, muscle and skin):

$$V_a\frac{dC_a}{dt} = Q_a(C_c - \frac{1}{K_{p,a}}C_a)$$

$$V_m\frac{dC_m}{dt} = Q_m\left(C_c - \frac{1}{K_{p,m}}C_m\right)$$

$$V_s\frac{dC_s}{dt} = Q_s(C_c - \frac{1}{K_{p,s}}C_s)$$

For bottom-up approaches (Models 1 and 2), the metabolism of bosentan into both hydroxyl bosentan and desmethyl bosentan was taken into consideration. PS_{act}, $PS_{dif,inf}$ and $CL_{int,met}$ were expressed by the following equations.

$$PS_{act} = \frac{In\ vitro\ V_{max,uptake} \times SF_{uptake}}{In\ vitro\ K_{m,uptake} + f_B C_{HEi}}$$

$$PS_{dif,inf} = In\ vitro\ PS_{dif,inf} \times SF_{uptake}$$

$$CL_{int,met} = \left(\frac{In\ vitro\ V_{max,met,OH}}{In\ vitro\ K_{m,met,OH} + f_H C_{HCi}} + In\ vitro\ CL_{met,OH,nonsaturable}\right.$$

$$\left. + \frac{In\ vitro\ V_{max,met,DES}}{In\ vitro\ K_{m,met,DES} + f_H C_{HCi}} + In\ vitro\ CL_{met,DES,nonsaturable}\right)$$

$$\times SF_{met}$$

where SF_{uptake} and SF_{met} were calculated based on 1.2×10^8 hepatocytes/g of liver, 24.1 g of liver/kg body, and 52.5 mg microsomal protein/g of liver (Davies and Morris, 1993; Iwatsubo et al., 1997). In the simulation analysis, the central compartment volume (V_c) was assumed to be 6.3 L/78 kg. In Model 2, the SF_{uptake}, SF_{met}, and V_c were optimized to fit the bosentan blood concentration profiles of the intravenous bosentan doses from 10 to 750 mg. In these analyses (Models 1 and 2), the values of $V_{max,uptake}$, $K_{m,uptake}$, $PS_{dif,inf}$, kinetic parameters representing the production of hydroxyl bosentan including $V_{max,met,OH}$, $K_{m,met,OH}$ and $CL_{met,OH,nonsaturable}$, and kinetic parameters representing the production of desmethyl bosentan including $V_{max,met,DES}$, $K_{m,met,DES}$, and $CL_{met,DES,nonsaturable}$ were fixed to the values from the *in vitro* kinetic parameters.

For top-down approaches (Models 3, 4 and 5), we performed simultaneous fitting analyses of the PBPK models that incorporate saturable processes for PS_{act}, $CL_{int,met}$ or both to bosentan blood concentration profiles. In Models 3, 4 and 5, the following parameters were optimized;

(1) Model 3

In vivo $V_{max,uptake}$, *in vivo* $K_{m,uptake}$, *in vivo* $PS_{dif,inf}$, *in vivo* $CL_{int,met,}$ and V_c

(2) Model 4

in vivo PS_{act}, *in vivo* $PS_{dif,inf}$, *in vivo* $V_{max,met}$, *in vivo* $K_{m,met}$ and V_c

(3) Model 5

In vivo $V_{max,uptake}$, *in vivo* $K_{m,uptake}$, *in vivo* $PS_{dif,inf}$, *in vivo* $V_{max,met}$, *in vivo* $K_{m,met}$ and V_c

The initial values of these fitting parameters were determined using the following methods: *in vivo* $V_{max,uptake}$ and *in vivo* PS_{dif} were extrapolated biologically from *in vitro* parameters described above; *in vivo* $K_{m,uptake}$ was set at the equivalent with *in vitro* $K_{m,uptake}$ values; *in vivo* PS_{act} was determined by calculating *in vivo* $V_{max,uptake}$/*in vivo* $K_{m,uptake}$ assuming a linear condition in which $f_B C_{HEi}$ was much lower than *in vivo* $K_{m,uptake}$; *in vivo* $CL_{int,met}$ was calculated by the sum of *in vivo* $V_{max,met,OH}/K_{m,met,OH}$, $CL_{met,OH,nonsaturable}$, $V_{max,met,DES}/K_{m,met,DES}$, and $CL_{met,DES,nonsaturable}$; *in vivo* $K_{m,met}$ was set at 5 μM according to *in vitro* $K_{m,met,OH}$ and $K_{m,met,DES}$; *in vivo* $V_{max,met}$ was determined by the calculation of *in vivo* CL_{met} and *in vivo* $K_{m,met}$; and V_c were set at 6.3 L/78 kg, respectively.

Supplementary text 2

Efforts to apply the PBPK model to reproduce pharmacokinetic profiles following oral bosentan dosing

The reported pharmacokinetic profiles of orally administered bosentan display deviations from dose-proportional behaviors, but in the opposite direction to the results of intravenously administered bosentan (Supplementary Figure 2). The dose-normalized AUCs of orally administered (as 100 ml aqueous suspension) showed a decreasing trend as the bosentan doses increased from 3 to 2,400 mg (Clin Pharmacol Ther 60: 124-37). This decreasing trend with oral bosentan dosing may arise from multiple mechanisms including the saturation in plasma protein binding, solubility, and/or uptake transporters (e.g. OATP2B1) expressed in the luminal side of enterocytes. To obtain mechanistic insights, we attempted to establish a PBPK model that can capture non-linear pharmacokinetic behavior of orally administered bosentan.

To develop a PBPK model for orally administered bosentan, several modifications were incorporated. First, the ADAM (Advanced Dissolution, Absorption and Metabolism) model was incorporated into the systemic PBPK model using SimCYP (version 16.0, SimCYP Ltd, Sheffield, UK, Supplementary Figure 3). The kinetic parameters are described in Supplementary Table 1 (V_{max} for CYP2C9 or CYP3A4, J_{max} for OATP1B1, and K_p scalar were re-optimized to reproduce the bosentan concentration-time profiles following intravenous bolus dosing). The following saturable components were also

incorporated into the PBPK model: i) hepatic efflux ($PS_{dif,eff}$) ii) intestinal solubility-pH profiles (reported in the interview form, Supplementary Figure 4), iii) intestinal efflux (by P-glycoprotein, obtained from Caco-2 permeability experiments with and without 100 μM verapamil), iv) intestinal uptake (by OATP2B1, obtained from the uptake study using HEK293 cells expressing OATP2B1). The possibility of supersaturation of bosentan in oral dosing solution (100 mL aqueous suspension) was also considered (the solubility of bosentan was described to be 0.01 mg/mL in the interview). Given each oral bosentan dose was given as 100 mL aqueous suspension, the fraction of API dissolved for each dose was set as described in Supplementary Table 2. Two cases of simulations were performed with the critical supersaturation ratio of 1 and 10, respectively, using SimCYP. For each case, the simulation was performed with J_{max} of OATP2B1 = 0, 5, 15, and 45 pmol/min, respectively in 100 virtual subjects generated from Sim-Healthy Volunteers.

The constructed PBPK model reasonably reproduced the non-linear pharmacokinetic profiles of intravenously administered bosentan (Supplementary Figure 5). However, it was not the case for orally administered bosentan, regardless of the consideration of the supersaturation of bosentan (Supplementary Figures 6 and 7). With low bosentan doses (3 – 100 mg), the simulation results were in a relatively good agreement with the reported profiles when J_{max} of OATP2B1 was set as 0 (i.e. no consideration of OATP2B1 uptake). However, the simulation results showed substantial deviations from

the reported profiles for high bosentan doses (600 - 2,400 mg), regardless of the consideration of apical uptake for OATP2B1.

Legends for Supplementary Figures

Supplementary Figure 1 Simulated Bosentan Concentration in Hepatocyte Compartment 1 by Model 3, 4 and 5

Supplementary Figure 2 Relationship between bosentan doses and the dose-normalized AUCplasma following intravenous (A) or oral (B) dosing
Error bars show the standard deviation.

Supplementary Figure 3 Structure of a PBPK model for orally administered bosentan
The ADAM (Advanced dissolution, absorption and metabolism) model was used for intestinal absorption of bosentan using SimCYP version 16.0.

Supplementary Figure 4 Solubility-pH profiles of bosentan
Square symbols represent the observed data in the interview form. Three colored curves represent simulated solubility-pH profiles; red, using in silico estimated pKa (= 4.0) and the intrinsic solubility (Sunionized, 0.0038mg/mL); green, using pKa (= 5.1) and Sunionized, (= 0.001mg/mL) described in the interview form; blue, using optimized pKa (= 5.4) and Sunionized, (= 0.0011mg/mL).

Supplementary Figure 5 (A) Mean plasma bosentan concentration-time profiles following intravenous dosing of various bosentan doses: 10 mg (black), 68 mg (purple), 308 mg (green), 500 mg (blue), and 904 mg (red), respectively. Solid symbols represent the observed mean values while the solid lines represent simulation results in 100 virtual subjects.
(B) Comparison of dose-normalized AUCs between the observed and predicted values
Red and blue symbols represent the simulated and observed values, respectively. Error bars show the standard deviation.

Supplementary Figure 6 Plasma concentration-time profiles of orally administered bosentan without consideration of supersaturation (critical supersaturation ratio = 1)
The Jmax values of OATP2B1 are set as 0 (A), 5 (B), 15 (C) and 45 (D) pmol/min, respectively. Solid symbols represent the observed mean values while the lines represent simulation results. Black, 3 mg; purple, 10 mg; blue, 30mg; red, 100 mg; black, 300 mg; purple, 600 mg; blue, 1,200 mg; red, 2,400 mg.

Supplementary Figure 7 Plasma concentration-time profiles of orally administered bosentan considering supersaturation (critical supersaturation ratio = 10)
The Jmax values of OATP2B1 are set as 0 (A), 5 (B), 15 (C) and 45 (D) pmol/min, respectively. Solid symbols represent the observed mean values while the lines represent simulation results. Black, 3 mg; purple, 10 mg; blue, 30mg; red, 100 mg; black, 300 mg; purple, 600 mg; blue, 1,200 mg; red, 2,400 mg.

Supplementary table 1

Input parameters for bosentan in SimCYP

Category	Parameters	Units	Value	Comments
Phys Chem and Blood Binding	molecular weight	g/mol	551.61	
	Log Po:w		3.4	
	pKa		Monoprotic Acid 5.4	Estimated from solubility-pH profile
	B/P		0.6	
	fraction unbound in plasma		0.02	
Absorption	Absorption model		ADAM model	
	$P_{eff,man}$	10-4cm/s	2.34	Calculated from in house Caco-2 permeability experiment data
	Formulation type		Suspension	
	Fraction API Dissolved	%	See Supplementary Table 1b	

	Aqueous Phase Solubility	mg/mL	Solubility-pH Profile	Solubility-pH profile is shown in Supplementary Table 1c
	Kinetic Solubility		Model 2	
	Critical Supersaturation Ratio		1, 10	1; no consideration of supersaturation 10; default value in SimCYP
Distribution	Distribution model		Full PBPK	
	Vss prediction method		Method 3	
	V_{ss}	L/kg	0.26	
	K_p scalar		3.54	Estimated using bonsentan i.v. concentration time profile
Elimination	Elimination model	Enzyme kinetics		
	HLM CYP2C9 K_m	µM	6.4	Set $K_{m,met,OH}$ value in Table 1
	HLM CYP2C9 V_{max}	pmol/min/mg protein	59.9	Estimated using bonsentan i.v. concentration time profile

	HLM CYP3A4 K_m	µM	4.8	Set $K_{m,met,DES}$ value in Table 1
	HLM CYP3A4 V_{max}	pmol/min/mg protein	67.4	Estimated using bonsentan i.v. concentration time profile
	CL_R	L/h	0.0864	Renal clearance described in Table 1 (0.144 L/h) * B/P (0.6) = 0.0864
	(Liver)			
	CL_{PD}	mL/min/million hepatocytes	0.00289	Set $PS_{dif,inf}$ value in Table 1
	fu_{IW}		0.0696	Set f_H value in Table 1
	OATP1B1 Km	µM	1.33	Set $K_{m,uptake}$ value in Table 1
	OATP1B1 J_{max}	pmol/min/million cells	179	estimated using bonsentan i.v. concentration time profile
Transport	Sinusoidal Efflux $CL_{int,T}$	µL/min/million cells	7.65	The difference between $PS_{dif,eff}$ and $PS_{dif,inf}$ ($PS_{dif,inf}$ * (γ - 1))
	(Intestine)			
	P-gp K_m	µM	4.09	in-house study
	P-gp J_{max}	pmol/min	124	in-house study

P-gp A	cm^2	1	in-house study
P-gp System		Caco-2	in-house study
			in-house study
Apical uptake K_m	µM	0.421	OATP2B1 was considered as an apical uptake transporter.
Apical uptake J_{max}	pmol/min	0, 5, 15, 45	
Apical uptake A	cm^2	1	
Apical uptake System		User	

Supplementary Table 2

Fraction of API dissolved value for each dose of bosentan

Bosentan dose (mg)	Fraction of API dissolved (%)
3	33
10	10
30	3.3
100	1.0
300	0.33
600	0.17
1200	0.083
2400	0.042

Supplementary Table 3

Solubility-pH profile of bosentan described in the interview form

pH	Solubility (mg/mL)
4	0.001
5	0.002
7.5	0.43
8	0.53
8.5	0.93

Supplementary Fig. 1

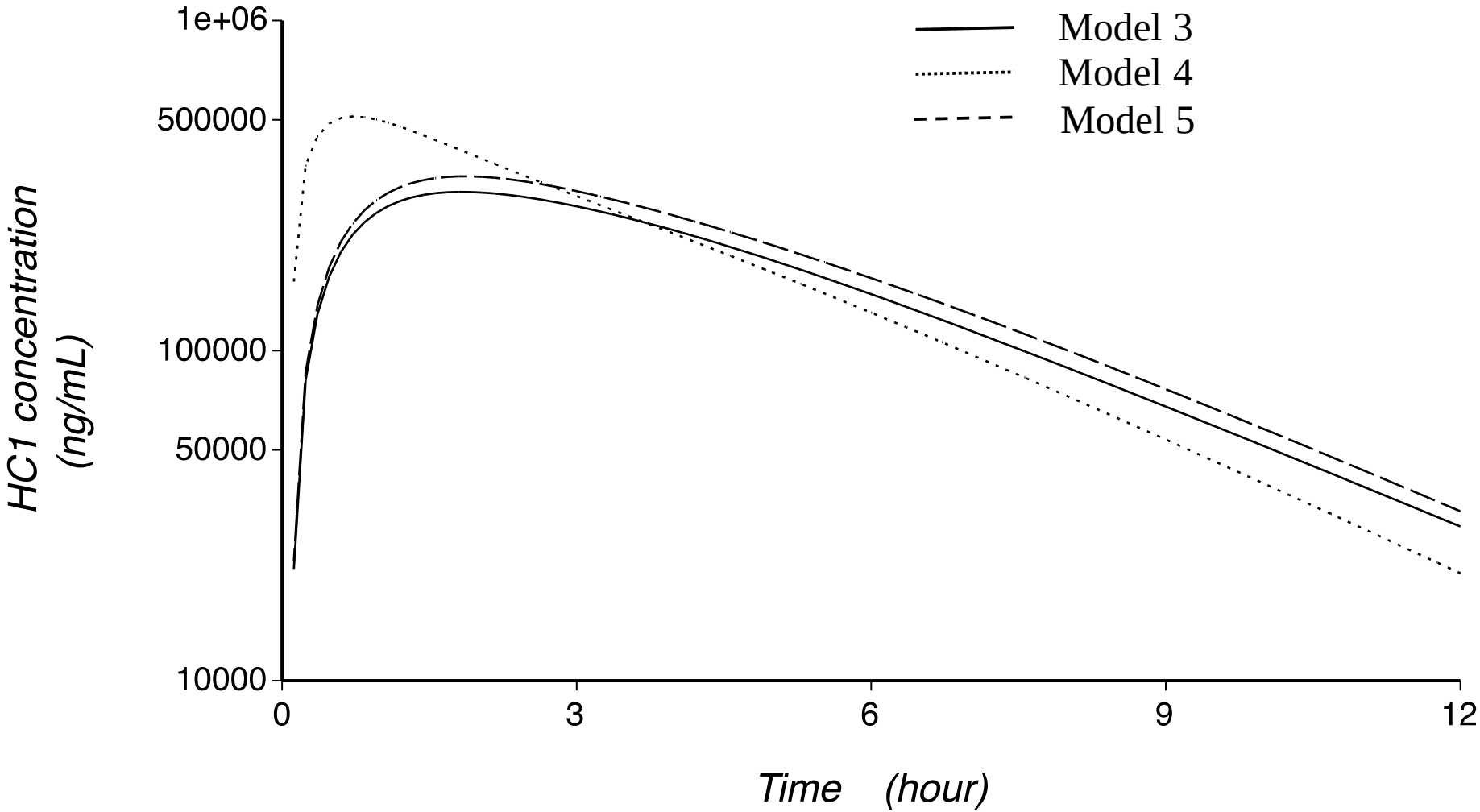

Supplementary Fig. 2

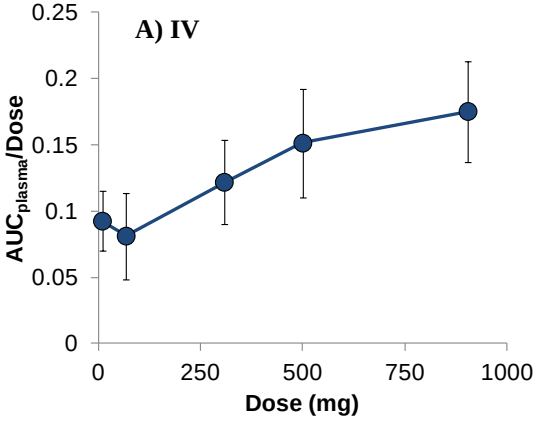

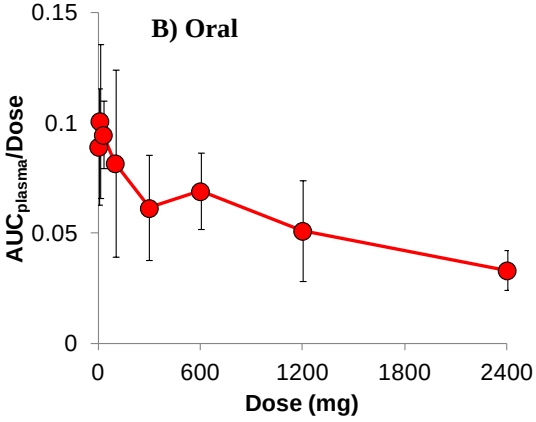

Supplementary Fig. 3

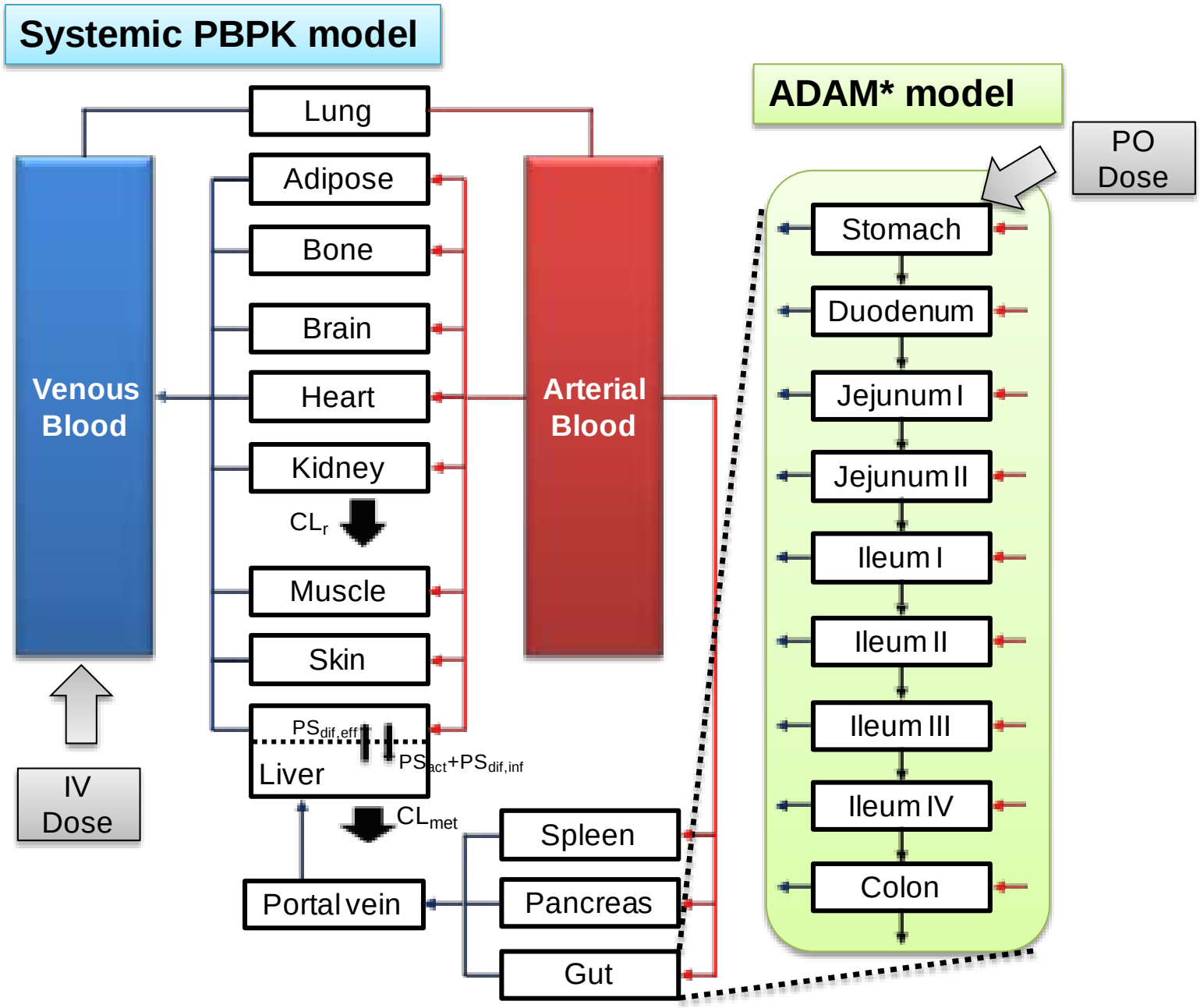

Supplementary Fig. 4

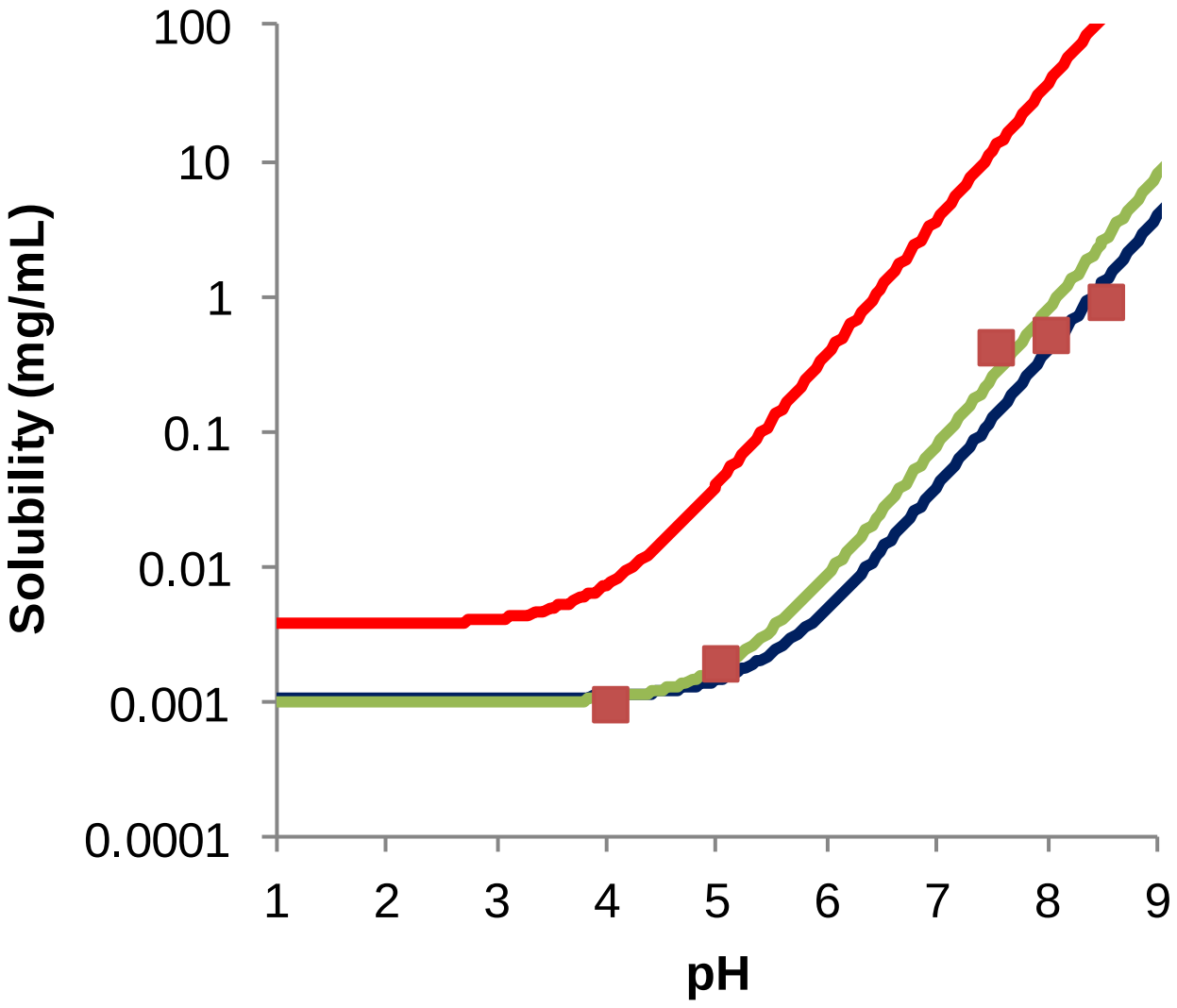

Supplementary Fig. 5

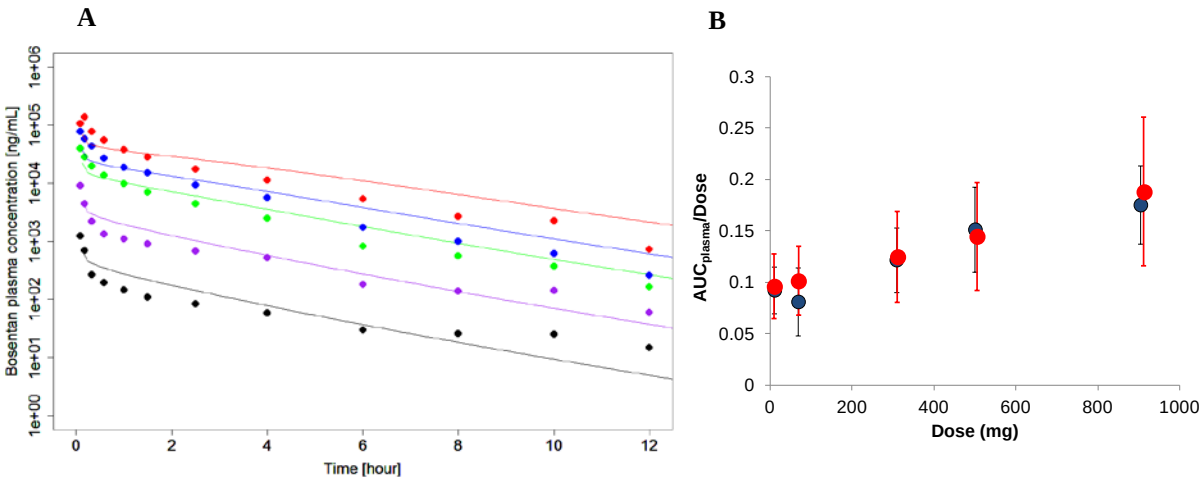

Supplementary Fig. 6

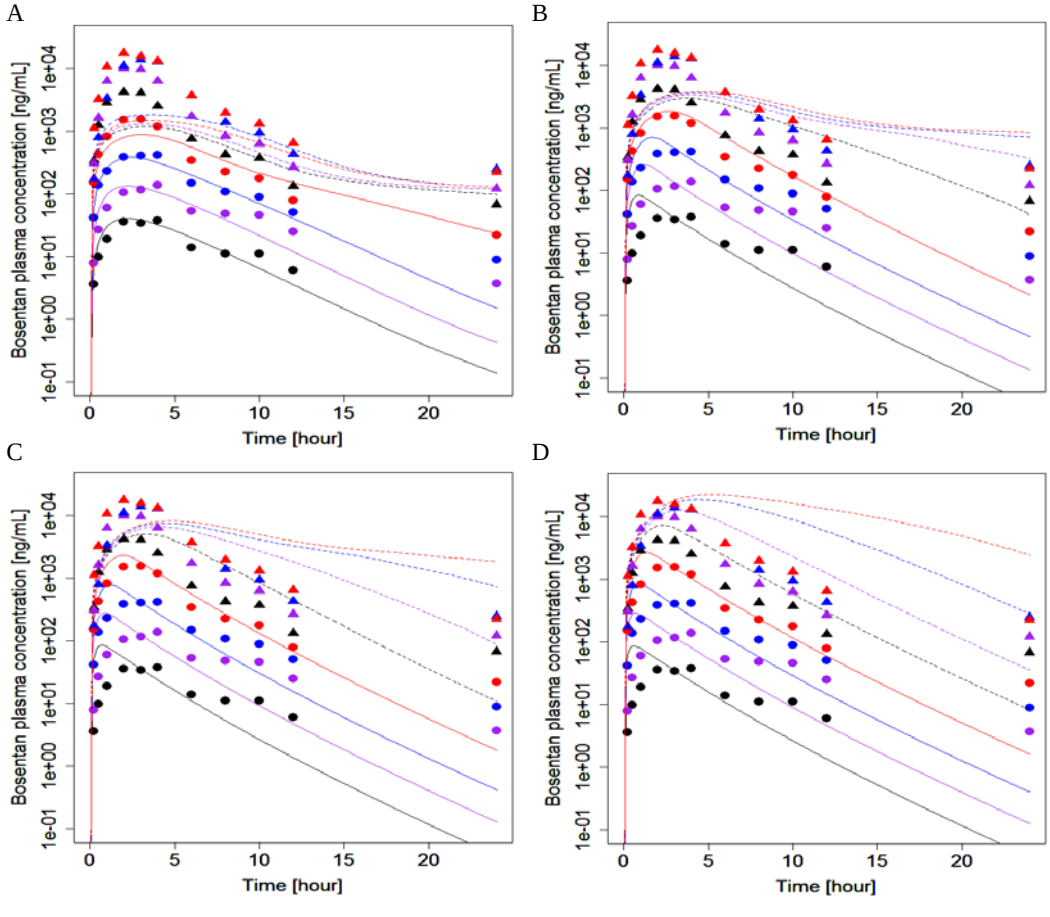

Supplementary Fig. 7